the B, C bands, with configuration $\pi^3\sigma$, it is the higher frequency member C which gets stronger as one goes toward Λ, S coupling. Incidentally, this gives an additional argument against the configuration $\pi^3\pi$ for the B, C bands.

All but one or two of the weakest of the Rydberg series observed by Price have now been accounted for, but expected series ending in $md\pi$ and $md\delta$ have not yet been identified.

In HCl, no Rydberg series have yet been identified, but only the B, C bands. However, the latter are accompanied[2] by "satellites" B', C' which repeat all the characteristics of the B, C bands at very slightly higher frequencies and with much lower intensities. The frequency interval $\nu_{C'}-\nu_{B'}$ and the intensity ratio $\nu_{C'}/\nu_{B'}$ are nearly the same (cf. Table II) as the corresponding quantities for B and C. The C' level, like the C level, is accompanied by a considerable amount of vibrational excitation, with the C' state showing a somewhat lower vibration frequency than the C state (2564 instead of 2670). Band B', like B, is accompanied by no vibrational excitation. The B', C' bands have P, Q, R structure, indicating a σ or a δ excited orbital. The term value is too large for $3d\delta$. The B', C' bands cannot be explained by an isotope effect (neither by DCl nor by $\mathrm{HCl}^{35,37}$). There seems to be no possibility but the following:

$$B'\colon\ (\sigma^2\pi^3,\ {}^2\Pi_{1\frac{1}{2}})c\sigma;\quad C'\colon\ (\sigma^2\pi^3,\ {}^2\Pi_{\frac{1}{2}})c\sigma,\qquad (7)$$

with $c\sigma$ identified as $4p\sigma$, which might perhaps help to account for the weakness of the bands. Since the bonding MO σ of Eqs. (1) and (2) may probably be considered for HCl as $3p\sigma$, $c\sigma$ may then be $4p\sigma$; this would explain why the $4p\sigma$ term value is larger (cf. Table I) than the $4p$ term value of the Cl atom.

MARCH 1 AND 15, 1942 PHYSICAL REVIEW VOLUME 61

Interpretation of the Methyl Iodide Absorption Bands Near λ2000

Robert S. Mulliken and Edward Teller
Ryerson Physical Laboratory, University of Chicago, Chicago, Illinois
*and Columbia University, New York, New York**

(Received January 16, 1942)

The theory of the types and structures of bands in an electronic transition in an axially symmetrical molecule of symmetry C_{3v} is discussed. This is applied to the methyl iodide B band system near λ2000, and it is shown that the two types of bands observed (strong and weak bands of pseudo-parallel type, and weak bands looking like perpendicular bands but of abnormally wide spacing) can both be explained. The pseudo-parallel bands are really electronic-allowed perpendicular bands, the narrowness of their structure resulting from an electronic angular momentum ζ_e in the upper state which we find from the data to be equal to 1.0. This ζ_e is explained by the electronic structure of the upper state, which behaves nearly like a Π state of a linear molecule. The weak widely-spaced bands are another kind of perpendicular bands made allowed by an interaction of the degenerate electronic state with a degenerate (e-type) vibration; they are $1\leftarrow 0$ and $0\leftarrow 1$ bands of such a vibration, and of a second similar vibration. Their spacing is approximately $1+\zeta_e+\zeta_v$ (ζ_v is the magnitude of the angular momentum of the degenerate vibration which is excited), as contrasted with a spacing $1-\zeta_e$ for the pseudoparallel bands (which correspond to the excitation, at most, only of totally-symmetrical vibrational states). Several molecular constants for the ground and excited electronic states are determined from the observational data (cf. Table I). The moment of inertia for rotations around the symmetry axis is found to be about 6 percent greater in the excited state than in the ground state. The theory of the coupling of spin, orbital angular momentum, and molecular vibration for various strengths of spin-orbit coupling is discussed. The actual nearly J, j-like coupling causes the $0\leftarrow 1$ band of the e vibration to appear with a relatively low intensity compared with the $1\leftarrow 0$ band of the same vibration.

1. INTRODUCTION

THE ultraviolet absorption spectra of the methyl halides begin at long wave-lengths with a continuum (A), followed by two adjacent and similar regions (B, C) of more or less discrete bands. Apparently the proximity of the A

---

* E. T. on leave of absence from The George Washington University. The work was begun while E. T. was Visiting Professor at the University of Chicago. Publication assisted by the Ernest Kempton Adams Fund for Physical Research of Columbia University.

continuum causes predissociation in B and C, since these show the most details in methyl iodide, where A is farthest away.

In methyl iodide, two types of B bands have been found.[1] In one type the bands are unresolved and fairly narrow and look like parallel bands. These include the strongest B bands (B_1, B_2, B_3, B_4), involving excitation of 0, 1, 2, and 3 quanta of the totally symmetrical CH_3 deformation frequency.[1] There are also several weaker narrow bands involving totally symmetrical $C-I$ vibrations. Some of the strong B bands are accompanied by one or two companions which may be transitions involving an extra quantum of one or another vibration in both upper and lower states. There are also some groups of bands, for example at 49,970–50,045 cm^{-1}, whose intensity decreases very rapidly with increasing temperature.[2] For this reason and because they cannot be explained by CH_3I vibrations, these bands may be ascribed to other molecules—perhaps to double CH_3I molecules, as mentioned by Henrici and Grieneisen and by Price.

The second type of B bands, including only broad weak bands, shows a series of roughly equidistant "lines" (mostly of about 20 cm^{-1} spacing), which may be interpreted as Q branches ($\Delta J=0$) of perpendicular bands ($\Delta K=\pm 1$, with a different K for each observed line). Every third line is stronger, as expected for rotation of the three hydrogen atoms of the methyl group around the symmetry axis with quantum number K. But a consistent interpretation of the whole B system presents difficulties.[1]

A comparative study of the hydrogen and alkyl halide spectra, however, points to rather definite conclusions as to the electron configurations involved.[3] It appears that the methyl halide B and C bands have normal (N) and excited (B, C) states which probably may best be described as follows (methyl group and halogen atom inner electrons are omitted):

$$N: (\sigma a_1)^2\pi^4,\ {}^1A_1;\ B: \{[(\sigma a_1)^2\pi^3,\ {}^2\Pi_{3/2}](\sigma^* a_1)\}_1;\quad C: \{[(\sigma a_1)^2\pi^3,\ {}^2\Pi_{1/2}](\sigma^* a_1)\}_1. \tag{1}$$

The meaning of the symbols in (1) is as follows: σa_1 is a $C-I$ bonding MO (molecular orbital) which is approximately of the axially symmetrical type σ characteristic of diatomic molecules, but more rigorously must be classified under the species a_1 of the symmetry C_{3v} characteristic of methyl iodide in its normal state. The symbol π refers to a nearly non-bonding orbital which probably differs little from a $5p\pi$ iodine AO;[4] strictly speaking this should be called πe corresponding to classification under the species e of C_{3v}. In states B and C one π electron has been excited to the large Rydberg orbital $\sigma^* a_1$. This orbital is perhaps predominantly $6s$ of iodine, but must extend into and considerably affect the CH_3 group, since only in that way[3] can we account for the considerable excitation of the CH_3 deformation and the decided lowering in the latter's frequency in the upper electronic state.

Because of the very strong spin-orbit coupling within the group π^3, the coupling between π^3 and $\sigma^* a_1$ is nearly J, j-like, so that there are essentially two states π^3, ${}^2\Pi_{3/2}$ and π^3, ${}^2\Pi_{1/2}$ of CH_3I^+, to either of which the $\sigma^* a_1$ electron is rather loosely coupled. The spin of the $\sigma^* a_1$ electron gives two levels with either of the core states ${}^2\Pi_{3/2}$ (levels with $\Omega=2$ and 1) and ${}^2\Pi_{1/2}$ (levels $\Omega=0^{\pm}$ and 1), but only the two levels with $\Omega=1$, one being the observed B and the other the observed C level, combine strongly with the ground state.[3] Ω here has the usual diatomic meaning; in the diatomic case one would speak of case c coupling. The wave functions of the two levels with $\Omega=1$ have the properties of mixtures of ${}^3\Pi_1$ and ${}^1\Pi$ functions. Combination of the B and C levels with N is due to the ${}^1\Pi$ part of the wave functions. From here on, we shall for the sake of simplicity think of both B and C upper levels as ${}^1\Pi$; this will lead to no error in the conclusions we shall reach in the earlier sections of the present paper. The effects of the mixed ${}^3\Pi_1$, ${}^1\Pi$ character of the B and C upper levels will be studied in the last section of this paper.

Strictly speaking, ${}^1\Pi$ is not a correct species label in the presence of C_{3v} symmetry, but ${}^1E$ should be used instead. Now Jahn and Teller

---

[1] For a review and references see H. Sponer and E. Teller, Rev. Mod. Phys. **13**, 76 (1941). This includes a tentative interpretation of the B bands as perpendicular bands.

[2] A. Henrici and H. Grieneisen, Zeits. f. physik. Chemie **B30**, 1 (1935).

[3] R. S. Mulliken, Phys. Rev. **61**, 277 (1942).

[4] See reference 2, footnote 9, in regard to the form of the π orbital of Eq. (1)

have shown[5] that orbitally degenerate electronic states (namely E states) of molecules of symmetry C_{3v} are not stable, but that, accompanied by distortion of the equilibrium configuration of the molecule, destroying the C_{3v} symmetry, such a state must split into two nondegenerate states. However, in CH_3I the H_3 group which is responsible for the C_{3v} symmetry and the ^1E classification is sufficiently remote from the iodine atom so that we may regard our $\pi^3\sigma^*$ state as a $^1\Pi$ perturbed by a weak C_{3v} external field. This perturbation and therefore also the Jahn-Teller splitting and accompanying distortion of the molecular configuration may then be minor effects.

If (1) is correct, the transitions from N to B and C are electronic-allowed transitions of perpendicular type, i.e., the electric moment of the electronic jump vibrates along a direction perpendicular to the $C-I$ axis. The strongest of the observed bands, looking like parallel bands, must then be perpendicular bands. It will now be shown that the apparent parallel structure can be satisfactorily explained if the B and C electronic states behave like little-perturbed $^1\Pi$ states.

2. STRUCTURE OF THE PSEUDO-PARALLEL BANDS

We have to consider a prolate-symmetrical-top molecule, with the usual features plus an electronic angular momentum along the axis. It is easily seen that the rotational term (energy/hc) is given by

$$\begin{aligned} F(K, J) &= B[J(J+1)-K^2]+AK_t^2+\cdots \\ &= B[J(J+1)-k^2]+A(k\mp\zeta_e)^2+\cdots, \qquad (2) \end{aligned}$$

where K_t is the magnitude of the nuclear top angular momentum in units of $\hbar$, ζ_e is that of the electronic angular momentum in the same units, and A and B are the usual rotational constants inversely proportional, respectively, to the small (unique) and to the large moment of inertia. The $-$ and $+$ signs in Eq. (2) respectively correspond to ζ_e parallel (Π^+ state) or opposed (Π^- state) to the vector k of total angular momentum around the symmetry axis; k can take on all positive and negative integral values including zero. (*Throughout the discussion*, we shall use small k as a quantity having sign as well as magnitude, but large K as $|k|$. In some but not all places in the discussion one can write equally well K or k.) For a pure $^1\Pi$ (or $^3\Pi_1$) state, $\zeta_e=1$, but by using the symbol ζ_e we can include the possibility that the magnitude of the electronic angular momentum has been somewhat reduced as a result of the C_{3v} symmetry. In the normal state of CH_3I, Eq. (2) holds with $\zeta_e=0$.

In a perpendicular transition, the selection rules are $\Delta J=0, \pm 1$ and Δk (or ΔK) $=\pm 1$. But if the transition is, as here, primarily an electron jump in which the quantum number k_e of the electronic angular momentum goes from zero to ± 1, the change in k is completely accounted for by the change in k_e and, if $\zeta_e=K_e=1$ for the upper state, there is no change in k_t. That is, $\Delta k=\Delta k_e=\pm 1$, $\Delta k_t=0$. Defining Δk as $k'-k''$, we have only $\Delta k=+1$ for the Π^+ upper state and $\Delta k=-1$ for the Π^- state. Transitions $\Delta k=-\Delta k_e=\pm 1$, giving $\Delta k_t=\mp 2$, are forbidden.

That the above rule is rigorous can be seen in the following way. A cyclic permutation of the three hydrogen nuclei must affect the wave functions of two combining states in the same way. Such a permutation may be carried out by rotating the molecule through the angle $2\pi/3$ around the figure axis, and then carrying out an opposite rotation (i.e., by $-2\pi/3$) on the electron wave function in the field of the fixed nuclei. The first operation multiplies the wave function by $e^{2k\pi i/3}$; the second operation leaves a $^1A_1$ electronic wave function unchanged, multiplies a $^1E^+$ function by $e^{-2\pi i/3}$ and a $^1E^-$ function by $e^{2\pi i/3}$. If the upper state is $^1E^+$ the permutation of the three protons will introduce the factor $e^{i(k'-1)2\pi/3}$ while in the $^1A_1$ lower state the factor $e^{ik''2\pi/3}$ appears. Equating the two exponentials and remembering that $|k'-k''|=1$, we find that for a $^1E^+$ (or a $^1\Pi^+$) upper state $k'=k''+1$. But since Δk is $k'-k''$ we have $\Delta k=+1$ for a $^1E^+$ upper state. By a similar consideration one finds $\Delta k=-1$ for a $^1E^-$ upper state. For $\Delta k_e\approx\pm 1$ we find $\Delta k_t=\Delta k-\Delta k_e\approx 0$.

Since the K part of the band structure depends mainly on ΔK_t, as is seen from Eq. (2) neglecting $-BK^2$ (which is small since B/A is about 1/8 for CH_3I), the bands here should have the appearance which parallel bands ($\Delta K=0$) have in the ordinary case where $\zeta_e=0$ and $\Delta K_t\equiv\Delta K$. The frequencies of the lines should be

---

[5] H. A. Jahn and E. Teller, Proc. Roy. Soc. **A161**, 220 (1937); including spin, H. A. Jahn, Proc. Roy. Soc. **A164**, 117 (1938).

given by:

$$\Delta k=+1:\ \nu=\nu_0+\nu_J-B'(k+1)^2 +A_0'[(k+1)-\zeta_e']^2+B''k^2-A_0''k^2,$$

$$\Delta k=-1:\ \nu=\nu_0+\nu_J-B'(k-1)^2 +A_0'[(k-1)+\zeta_e']^2+B''k^2-A_0''k^2,$$

where ν_J represents the usual functions of J corresponding to P, Q, and R branches ($\Delta J=-1$, 0, $+1$), k refers always (in accordance with the usual convention) to the lower state in the transition, the primes and double primes refer in the usual way to upper and lower states, and the subscripts zero in A denote zero vibrational quantum numbers. The ν equations for both $\Delta k=+1$ and $\Delta k=-1$ can be reduced to the form

$$\nu=[\nu_0-B'+A_0'(1-\zeta_e')^2]+\nu_J \pm 2[A_0'(1-\zeta_e')-B']K+(A_0'-A_0'')K^2. \quad (3)$$

The + and − signs, respectively, correspond to an r branch ($K'-K''=+1$) and a p branch ($K'-K''=-1$).* If $\zeta_e'=1$, and B' is neglected compared with A_0', Eq. (3) becomes identical with the formula for ordinary parallel bands. So long as B' and $1-\zeta_e'$ are small, the appearance under incomplete resolution of bands corresponding to Eq. (3) should be similar to that of parallel bands. The methyl iodide B and C bands of the first type seem to be in harmony with this description.

3. THEORY AND STRUCTURE OF THE WIDELY SPACED BANDS

We turn now to the second type of B bands which look like widely-spaced but otherwise normal perpendicular bands. Assuming the strongest pseudo-parallel band (B_1) to be a vibrationless transition, we can interpret the weak, strongly temperature-dependent band at about 880 cm^{-1} toward the red as a 0←1 transition of an e-type (π-like) vibration superimposed upon the electronic transition. In fact, a perpendicular band has been observed at 885 cm^{-1} in the infra-red spectrum.[6] One can visualize the vibration of this frequency roughly as a bending vibration of the C−I bond with respect to the figure axis of the CH_3 group. Another ultraviolet band of perpendicular appearance shifted from B_1 toward *higher* frequencies by 780 cm^{-1} may be interpreted as the 1←0 transition of the same bending vibration superimposed upon the electronic transition.

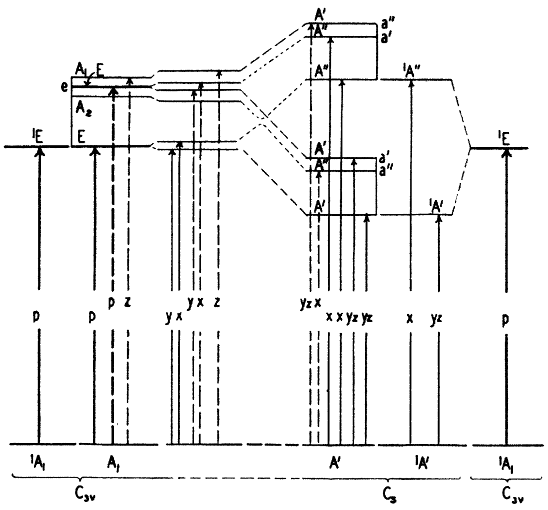

FIG. 1. *Left of diagram:* Allowed transitions for a CH_3I molecule with a $^1A_1$ lower and ^1E upper electronic state, with no vibration in the lower state and either no vibration or one quantum of e-type vibration in the upper state, assuming symmetry C_{3v} with z axis as symmetry axis. *Right of diagram:* Corresponding energy levels and transitions assuming symmetry C_s (one plane of symmetry passing through the C and I atoms and one hydrogen atom) for the upper electronic state, with yz plane as symmetry plane. *Middle of diagram:* Shows correlations between symmetry C_s and C_{3v}; at left of middle, distortion of C_{3v} symmetry only slight. Throughout the diagram, the symbols with left-hand superscript refer to electronic states, small-letter symbols refer to the vibration mode excited (if any), and the capital-letter symbols without left-hand superscript refer to vibronic states. Electronic-allowed transitions are shown by full vertical lines, vibronic-allowed transitions by dashed vertical lines; directions of polarization are indicated by letters x, y, z (p stands for x and y).

According to the simplest application of the Franck-Condon principle for polyatomic molecules, both bands described in the previous paragraph should be forbidden. For a degenerate upper electronic state of the E type in a molecule of the symmetry C_{3v}, however, the transitions become allowed. As we shall see, they can even become quite strong.

We consider first the 1←0 vibrational transition. In the lower electronic state the electronic wave function is of the $^1A_1$ type and the vibra-

---

* In the r branch, each K corresponds to a pair of k transitions of equal frequency, one a $\Delta k=+1$ transition with k positive, the other a $\Delta k=-1$ transition with k negative; and similarly for the p branch except that the signs of k are reversed. ***Added in proof:*** In Eqs. (3), (5), (6), (8), and (9), $(A_0'-A_0''-B'+B'')$ should appear instead of $(A_0'-A_0'')$; the B terms were omitted through an oversight.

[6] W. H. Bennett and C. F. Meyer, Phys. Rev. **32**, 888 (1928).

tional wave function (in the assumed absence of vibrational excitation) is likewise A_1. In the upper electronic state we may distinguish two sub-states E^+ and E^- both belonging to the degenerate approximately-$^1\Pi$ state. The E^+ and E^- states transform, respectively, like $e^{i\phi}$ and like $e^{-i\phi}$ under rotations of the molecule through the angles $\frac{1}{3}2\pi$ or $\frac{1}{3}4\pi$. The vibrational wave function in the excited state is similarly of the species E, and again we may distinguish two sub-states E^+ and E^-.

On combining the ^1E electronic with the E vibrational state, there must result,[1] according to group theory for symmetry C_{3v}, a $^1A_1$, a $^1A_2$, and a ^1E vibronic state (cf. Fig. 1). These three states are, respectively, analogous to the $^1\Sigma^+$, $^1\Sigma^-$, and $^1\Delta$ states which in a linear molecule would result from the interaction of a $^1\Pi$ electronic state and a Π vibrational state, for example a state with one quantum of a bending vibration. Combination with the vibrationless ground state (vibronic species $^1A_1$) is allowed, according to the vibronic selection rules, for both the $^1A_1$ and the ^1E upper vibronic states. The transition to the upper $^1A_1$ should give a weak parallel band. Such a vibronic-allowed electronic-forbidden transition draws its intensity from other electronic-allowed transitions of the same vibronic type.[1] In the present instance, this intensity should probably be taken mainly from the D bands, which lie at slightly higher frequencies than the B and C bands, are comparable to the latter in intensity, and are probably an electronic-allowed transition of the $^1A_1 \leftarrow {}^1A_1$ type.[3]

In detail, the $^1A_1$ and $^1A_2$ upper vibronic state wave functions are 50, 50 mixtures of wave functions E^+e^- and E^-e^+. (*Here and elsewhere in this paper we shall use large E for electronic and small e for vibrational E wave functions.*) On the other hand, the ^1E upper vibronic state is a degenerate state with components E^+e^+ and E^-e^- having transformation properties respectively like those of E^- and E^+ electronic states. This means that our initial pure E^+e^+ state becomes somewhat mixed with, among others, various vibrationless E^- electronic states (analogous to both $^1\Pi$ and $^1\Delta$ states of a linear molecule); simultaneously, E^-e^- is mixed with E^+. This permits a very weak vibronic-allowed combination with the ground level, in the form of a perpendicular band which should be approximately superimposed on the parallel band discussed in the preceding paragraph.

Actually the perpendicular band can be much stronger than the parallel band because of an effect similar but additional to the simple vibronic mixing just discussed. The effect consists in a mixing of the E^+e^+ state with the vibrationless electronic B state E^-, and similarly of E^-e^- with E^+. This is a result of the same mechanism which leads to the splitting of orbitally degenerate electronic states under the influence of non-totally-symmetrical deformations (in the present case e-type deformations) of the nuclear configuration. Such deformations cause changes in the electronic wave functions, and for small displacements one can calculate these with the help of perturbation theory. For an E electronic state the perturbing potential has non-diagonal matrix elements between the E^+ and E^- wave functions. These matrix elements give rise to a splitting of the degenerate electronic state, and as a general rule this splitting increases linearly with the nuclear displacement. Thus the symmetrical configuration no longer corresponds to a minimum of the energy. One finds, instead, new equilibrium positions. But if the e-type displacement gives rise only to ***small*** non-diagonal matrix elements, the distances of the new equilibrium positions from the symmetrical configuration may be smaller than the zero-point amplitudes of the e-type vibrations. In that case it is justifiable to consider non-diagonal matrix elements between vibronic states rather than non-diagonal matrix elements between electronic states. Then the E^+e^+ wave function will be mixed with the vibrationless E^- wave function of the same electronic state (i.e., the B state). Because of the close proximity of this particular E^- state to the E^+e^+ state, its effect is great. The selection rule forbidding transitions from the ground state to the e vibrational state of an upper electronic state would be completely removed if the distance of the actual equilibrium configuration from the symmetrical configuration should become equal to or should exceed the zero-point amplitude of the e vibration.

The way in which the $Ee \leftarrow A_1$ transition becomes allowed as the influence of the e deformations on the E electronic state is increased is illustrated in Fig. 1. The right half of Fig. 1 indicates schematically how the energy levels corresponding to the vibrationless E and to the Ee states might be arranged if the influence of such deformations is so strong that the equilibrium configuration differs from the original C_{3v} configuration more strongly than would correspond to zero-point vibrational displacements. Both the electronic and the vibrational state are split; Fig. 1 shows a possible arrangement of the levels, and the allowed transitions, if the new equilibrium configurations have symmetry C_s. Transitions to both the vibrationless electronic states ${}^1A'$ and ${}^1A''$ resulting from the splitting of ${}^1E$ are about equally allowed, and further, for each of these a band corresponding to (half of) our $1\leftarrow0$ band is now strongly electronic-allowed, since one component of the split e vibrational state is now of the totally symmetrical species a' of the new symmetry. (In addition, two weak bands going to the other component a'' of the split e state are vibronic-allowed.)

If, on the other hand, the influence of the e-type deformations is much smaller, the arrangement of energy levels may be nearly the same as in the unperturbed C_{3v} case (cf. Fig. 1, left side of middle). This would correspond to a much smaller mixing between the E^+e^+ and E^- states and a much lower intensity of the $1\leftarrow0$ band. A relatively small amount of mixing is sufficient to account for the actually observed intensity in the methyl iodide $1\leftarrow0$ band.

The $0\leftarrow1$ transition can be explained by the same kind of mixing. Since the vibrationless E^+ electronic state is mixed to some extent with E^-e^-, a combination with the vibrating ground state A_1e^- becomes permitted. Similarly, the E^- upper state, through mixing with E^+e^+, is able to combine with A_1e^+.

To obtain the rotational structure of the $1\leftarrow0$ vibrational band of the B system, we consider the rotational energies of the E^+e^+ and E^-e^- states. These are

$$B'[J(J+1)-k^2]+A_1'[k\mp(\zeta_e'+\zeta_v')]^2+\cdots. \quad (4)$$

This is essentially the same as Eq. (2) for the vibrationless electronic state with the sole difference that here the quantity ζ_v' has been included.* This ζ_v' measures the magnitude of the average angular momentum of the one-quantum vibrational state e in the excited electronic state, in units of h. In Eq. (4), the upper $(-)$ sign belongs to E^+e^+, the lower $(+)$ to E^-e^-.

In discussing the rotational structure of the $(0\leftarrow0)$ band we have seen that, in the $E^-\leftarrow A_1$ and $E^+\leftarrow A_1$ transitions, respectively, k decreases or increases by one unit. The same must be true for the $E^+e^+\leftarrow A_1$ and $E^-e^-\leftarrow A_1$ transitions, since these are made allowed only by the mixing of E^+e^+ with E^-, and of E^-e^- with E^+. Thus we have E^+e^+ giving only $\Delta k=-1$ here, and E^-e^- giving only $\Delta k=+1$. Hence the frequencies of the lines in the $1\leftarrow0$ band should be

$$\begin{aligned}\Delta k=-1:\ \nu&=\nu_0+\nu_J-B'(k-1)^2\\&\quad+A_1'[(k-1)-\zeta_c'-\zeta_v']^2+B''k^2-A_0''k^2,\end{aligned}$$

$$\begin{aligned}\Delta k=+1:\ \nu&=\nu_0+\nu_J-B'(k+1)^2\\&\quad+A_1'[(k+1)+\zeta_e'+\zeta_v']^2+B''k^2-A_0''k^2.\end{aligned}$$

Both equations can be reduced (cf. Eq. (3)) to the form

$$\begin{aligned}\nu&=[\nu_0-B'+A_1'(1+\zeta_e'+\zeta_v')^2]+\nu_J\\&\quad\pm2[A_1'(1+\zeta_e'+\zeta_v')-B']K+(A_1'-A_0'')K^2. \quad (5)\end{aligned}$$

The $+$ and $-$ signs correspond to an r and a p branch, respectively.

The form of Eq. (5), i.e., $\nu=a+\nu_J\pm2bK+cK^2$, is exactly the same as for ordinary perpendicular bands. If $B'-B''$ is negligible, as seems to be true for the B system of CH_3I, the term ν_J represents for each K value an intense line-like Q branch ($\Delta J=0$, $\nu_J=0$), together with spread-out P and R branches which with ordinary dispersion should appear merely as weak unresolved background. All this is the same as for an infra-red perpendicular band,[7] where for a $1\leftarrow0$ transition

$$\begin{aligned}\nu&=[\nu_0+A_1''(1-\zeta_v'')^2-B']+\nu_J\\&\quad\pm2[A_1''(1-\zeta_v'')-B']K+(A_1''-A_0'')K^2. \quad (6)\end{aligned}$$

The only novel feature in Eq. (5) is the very large spacing of approximately $2[A'(1+\zeta_e'+\zeta_v')-B']$

---

* The identity in symbols between the *coefficient* A_1 and the *species* A_1 is purely accidental.

[7] See M. Johnston and D. M. Dennison, Phys. Rev. **48**, 868 (1935) for discussion of theory of ζ_v and determination of moments of inertia in the methyl halides.

between successive lines of the p or r branch. This is exactly what we need to explain the hitherto puzzling[1] fact that the observed 1←0 ultraviolet band has larger spacings than occur in any of the infra-red perpendicular bands of CH_3I, larger even than when ζ_v in Eq. (6) is negative (ζ_v in the methyl halides has values between the limits $+1$ and -1).[7] A quantitative study of the data on the 1←0 and 0←1 ultraviolet bands will be given below.

To obtain the predicted structure of the 0←1 band we consider the $E^+ \leftarrow A_1e^-$ and the $E^- \leftarrow A_1e^+$ transitions. The rotational energy of the upper state is given by Eq. (2), that of the lower state by

$$B''[J(J+1)-k^2]+A_1''(k\mp\zeta_v'')^2+\cdots. \quad (7)$$

Since the transition draws its intensity from $E^+e^+ \leftarrow A_1e^+$ and $E^-e^- \leftarrow A_1e^-$, Δk must be -1 for $E^+ \leftarrow A_1e^-$ just as for $E^-e^- \leftarrow A_1e^-$, and similarly, $+1$ for $E^- \leftarrow A_1e^+$. Hence

$$\Delta k=-1:\ \nu=\nu_0+\nu_J-B'(k-1)^2 \\ +A_0'[(k-1)-\zeta_e']^2+B''k^2-A_1''(k+\zeta_v'')^2,$$

$$\Delta k=+1:\ \nu=\nu_0+\nu_J-B'(k+1)^2 \\ +A_0'[(k+1)+\zeta_e']^2+B''k^2-A_1''(k-\zeta_v'')^2,$$

which can both be reduced to

$$\nu=[\nu_0-B'+A_0'(1+\zeta_e')^2-A_1''\zeta_v''^2]+\nu_J \\ \pm 2[A_0'(1+\zeta_e')+A_1''\zeta_v''-B']K \\ +(A_0'-A_1'')K^2, \quad (8)$$

with the + and − signs for the r and p branches, respectively. Here again, in agreement with the observed 0←1 band, the structure is the same as that of infra-red perpendicular bands except for the very large spacing, which is predicted to be approximately $2[A_0'(1+\zeta_e')+A_1''\zeta_v''-B']$.

In connection with the study of the experimental data on the 0←0, 1←0, and 0←1 bands, it will be useful to know what is expected for the location and structure of the 1←1 band ($E^+e^+ \leftarrow A_1e^+$ and $E^-e^- \leftarrow A_1e^-$). Using Eqs. (4) and (7) for the upper and lower states, respectively, one obtains

$$\nu=\{\nu_0-B'+A_1'[1-(\zeta_e'+\zeta_v')]^2-A_1''\zeta_v''^2\} \\ +\nu_J\pm 2[A_1'(1-\zeta_e'-\zeta_v')+A_1''\zeta_v''-B']K \\ +(A_1'-A_1'')K^2, \quad (9)$$

with the + and − signs for the r and p branches, respectively. If $\zeta_e'\approx 1$ and $\zeta_v'\approx\zeta_v''$, the coefficient of K is nearly zero, so that the band should be of pseudo-parallel type like the 0, 0 band.

4. ANALYSIS OF EXPERIMENTAL DATA ON 0→1 AND 1→0 BANDS

In this and the next section we seek to interpret the available data with particular reference to the 0←0, 1←0, and 0←1 B bands, and to obtain empirical values of various molecular constants and coefficients (ζ's and A's). In order better to understand the observed band structures, Fig. 2 has been constructed. This shows the K structures of the vibrationless and the 1-quantum e levels for the normal and the excited electronic state, together with the low-K lines of the p and r branches of the various bands which are possible (1←0 infra-red, 1←0, 0←0, 1←1, and 0←1 ultraviolet) for transitions among these levels. The J structure of the levels and bands is omitted. The positions of the various K levels in Fig. 2 have been drawn according to Eqs. (2), (4), (7), *with the schematic simplication that all coefficients A have been assumed equal.* Values of B/A, ζ_v'', ζ_v' and ζ_e' obtained from the analysis given below have been used.

Because of the presence of three equivalent hydrogen nuclei in CH_3I, every third K level has a doubled statistical weight corresponding to resultant nuclear spin 3/2 (weight 4) as compared with spin 1/2 with weight 2 for the remaining levels. The levels with doubled spin weight, and the corresponding transitions, which all have doubled intensity, have been determined[8] and are shown in Fig. 2 by heavy lines. The vertical lines representing the transitions in each band are arranged horizontally with spac-

---

[8] Cf. E. Bright Wilson, Jr., J. Chem. Phys. **3**, 283 (1935). Wilson's Table XII gives the *total* weight (nuclear spin weight, times number of levels of given K, times weight due to K-doubling) for each K value. Figure 2 here shows the distribution more in detail. For the ground state A_1 there is a single $K=0$ level with spin weight 4, and a set of levels $K>0$ with double weight because of $k=\pm K$ and in addition a spin weight two, or four in the case of levels where K is a multiple of three. For the states A_1e and E, the $K=0$ level is double (i.e. two $K=0$ levels probably very close together) and has a spin weight of two, or a total weight of four, as given by Wilson. Then there are *two* $K=1$ levels rather far apart, with a spin weight of four for one and two for the other, and each having a further double weight because of $k=\pm K$; thus the total weight of both $K=1$ levels together is 12, in agreement with Wilson. The Ee state is similar to A_1e and E, but the strongly weighted levels are differently distributed.

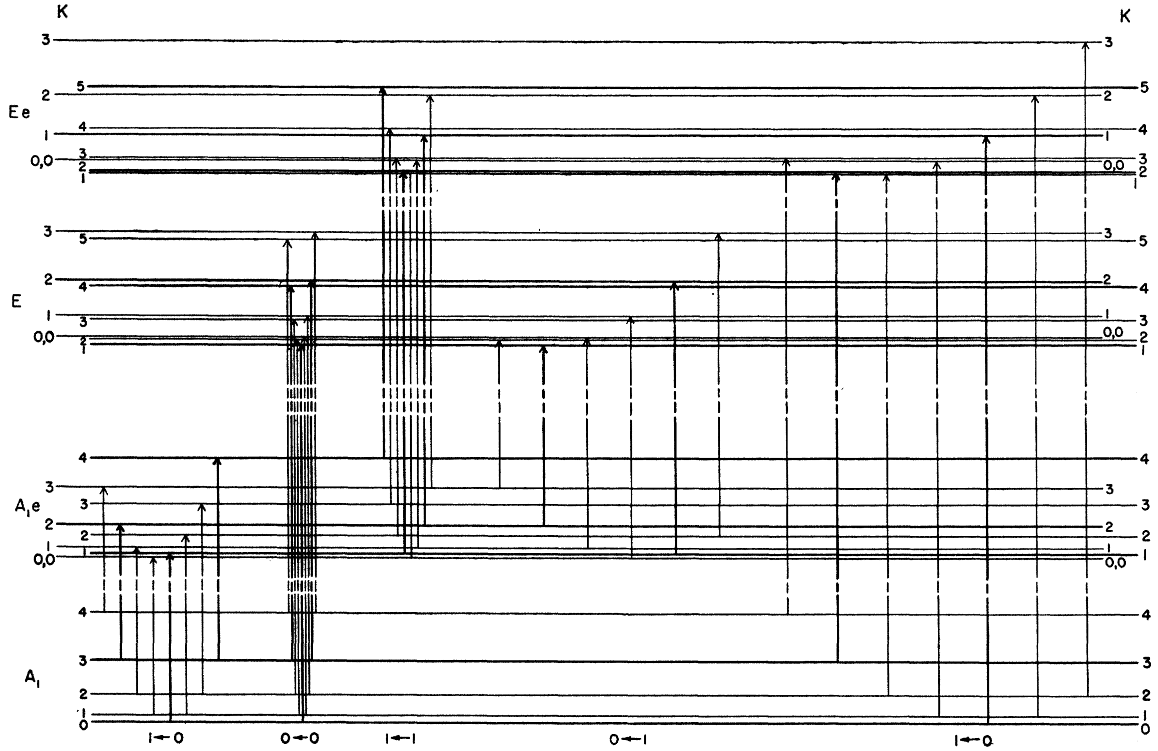

FIG. 2. Energy levels of the K rotation for the ground (A_1) and B excited (E) electronic states of CH_3I, with and without vibration of the type e; and allowed transitions among these levels. The changes in vibrational quantum number for the five possible bands are given at the bottom of the figure. Levels with double spin weight, and corresponding transitions, are shown by heavy lines. See second paragraph of Section 4 for further explanation.

ings proportional to those given by the appropriate equation for the band (cf. Section 3). Thus from the figure, keeping in mind that for thermal equilibrium the absorption intensities (aside from the effect of spin weight) should fall off with increasing K from a maximum at $K=0$, one can readily visualize the appearance of each band.

Referring now to the data of Henrici and Grieneisen[2] on the 0←1 ultraviolet band, and especially to their Fig. 1, one can immediately identify their strongest observed line at $\nu=48{,}878$ cm^{-1} with $r(1)$ of the 0←1 band of Fig. 2. With this identification, one can proceed to fit the set of ten observed lines in this band to an equation of the form of Eq. (8). Since the observed "lines" are Q branches ($\Delta J=0$), and if we assume $B'=B''$, the term ν_J in Eq. (8) drops out. [That $B'=B''$ is nearly true is indicated by the narrow symmetrical appearance[2] of the observed Q branches; also by the fact that the frequency of the totally-symmetrical C–I vibration does not differ much in the upper and lower electronic states.[2]] The following equation reproduces the data within an average deviation of less than ± 1 cm^{-1}:

$$\nu=48{,}858\pm 20.5K-(\tfrac{1}{3})K^2. \qquad (10)$$

According to Eq. (8), the coefficient of K in Eq. (10) should be equal to $2[A_0'(1+\zeta_e')+A_1''\zeta_v''-B']$, and the coefficient of K^2 to $(A_0'-A_1'')$.

With the help of infra-red data, we can now evaluate ζ_e'. Assuming $B'=B''$, B' can be obtained approximately from unresolved infra-red parallel bands; the value is 0.28 ± 0.02 cm^{-1}.[9] Then from the three infra-red perpendicular fundamental bands, $A_0''=5.08$ ($\pm$ about 0.3) cm^{-1} is obtained; unfortunately this is not very accurate.[9] Next we make use of the empirical

---

[9] The values of B_0'' and A_0'' are obtained from the moments of inertia $I_B=99\times 10^{-40}$ and $I_A=5.44\times 10^{-40}$ given in reference 7.

equation[6]

$$\nu = 885.15 + 7.70K + 0.032K^2 \tag{11}$$

for the infra-red 1←0 perpendicular band of Fig. 2. The constants of Eq. (11) enable use to determine $A_1'' = 5.11$ (± about 0.3), then $\zeta_v'' = 0.19$, and finally $\nu_0 = 882.09$, for Eqs. (6), (11). Unfortunately the uncertainty in ζ_v'' is rather large (perhaps ±0.05).

Using the coefficient of K^2 in Eq. (10), we now obtain $A_0' = 4.78$ (± about 0.3). We can then evaluate ζ_e' and find the value 0.998, in excellent agreement with our original expectation that ζ_e' should be nearly 1. Unfortunately, however, there is an empirical probable uncertainty of about ±0.1 in our value; this goes back to the uncertainty in A_0''.

The value of ν_0 in Eqs. (8), (10) can now be determined as 48,839.3. Adding this to $\nu_0 = 882.1$ for the 1←0 infra-red band, we obtain 49,721.4 as a predicted ν_0 for the 0←0 ultraviolet transition. As we shall see below, this is in good agreement with what is obtained by a direct interpretation of the structure of that band. This agreement gives support to our interpretation of the 0←1 ultraviolet band, and also indicates that by good luck, the error in the value of A_0'' we have used, and so in the values of ζ_v'' and ζ_e', is well inside our estimates.

For the 1←0 ultraviolet band,[10] assuming that the strongest of the sixteen observed *p* and *r* transitions, with $\nu = 50{,}492$ cm^{-1}, has $K = 0$ as would be expected according to Fig. 2, we find

$$\nu = 50{,}492\tfrac{1}{3} \pm 21\tfrac{2}{3}K - \tfrac{1}{3}K^2. \tag{12}$$

By comparison with the corresponding theoretical Eq. (5), and making use of the values of A_0'', B', and ζ_e' already determined, we find $A_1' = 4.75$ and $\zeta_v' = 0.34$, the latter a not unreasonable value. We further determine $\nu_0 = 50{,}466.6$.

The constants and coefficients so far determined are summarized in Table I. Two results of some interest are obvious. From the ν_0 values, the perpendicular frequency we have been discussing is seen to have the magnitude 882 cm^{-1} in the lower and 745 cm^{-1} in the upper state. The latter figure is considerably lower than the value 780 cm^{-1} obtained by Henrici and Grieneisen by subtracting ν of the 0←0 band from ν for $K = 0$ of the 1←0 band. The change is due to the large correction to ν_0 in the constant term in Eq. (5).

The second interesting result is the 6 percent decrease in A during excitation to the upper level of the ultraviolet bands. (Note that the *change* in A is accurately known.) This means a 6 percent increase in the moment of inertia around the symmetry axis and probably corresponds to a spreading out of the CH_3 umbrella. This is in harmony with the rather strong excitation of the CH_3 totally-symmetrical deformation vibration in the main series of bands B_1 to B_4, and with the 12 percent decrease in the frequency of this vibration in going to the upper state.

5. INTERPRETATION OF DATA ON 0←0, 1←1, AND OTHER BANDS

Putting the constants listed in Table I into Eqs. (3) and (9), it is possible to predict the exact structures of the 0←0 ($E \leftarrow A_1$) and the 1←1 ($Ee \leftarrow A_1e$) bands. If one assumes $B' = B''$ and $\Delta J = 0$, the equations are:

$$0\leftarrow 0 \text{ band}: \nu = 49721.1 \pm (-0.54)K - \tfrac{1}{3}K^2, \tag{13}$$

$$1\leftarrow 1 \text{ band}: \nu = 49584.6 \pm (-1.84)K - 0.36K^2. \tag{14}$$

The constant terms equal $\nu_0 - 0.28$ and $\nu_0 - 0.72$ in Eqs. (13) and (14), respectively. The + and −

TABLE I. Constants of CH_3I levels. A_1 refers to the ground electronic state, E to the excited state B; e refers to the degenerate vibration whose frequency is 885 cm^{-1} in the ground state.

State	ν	A	B	ζ_e	ζ_v
A_1	0.0	5.08	0.28	0.00	0.00
A_1e	882.1	5.11	0.28	0.00	0.19
E	49721.4	4.78		1.00	0.00
Ee	50466.6	4.75		1.00	0.34

---

[10] We have used the data of reference 2. It is possible that $K = 0$ is 50,554, which is nearly as strong as 50,492: cf. Figs. 1 and 2 of reference 2, also Table I and Fig. 3 of the paper of Scheibe, Povenz, and Linström [Zeits. f. physik. Chemie **B20**, 288 (1933)]. But most probably 50,492 has $K = 0$ and the relatively high apparent strength of 50,554 and the other *rQ* transitions as compared with corresponding *pQ* transitions can be explained by the effects of closer packing in the background of *P* and *R* branches in the *r* than in the *p* range. Some slight doubts as to the empirical correctness of our Eq. (12) are also raised by the fact that Scheibe, Povenz, and Linström, although generally agreeing fairly well with Henrici and Grieneisen, give ν values lower than those of the latter authors by amounts ranging from 25 to 38 cm^{-1} in the case of the 1←0 band.

signs correspond as usual to r and p branches, but the initial directions of these branches are reversed by the extra $-$ sign. A plot of Eq. (13) shows a head at the p line $K=1$ with $\nu=49721.3$, all the other K lines being at lower frequencies. All strong lines are crowded near this head, while weaker lines, with increasing spacing, tail off toward longer wave-lengths. These lines are of course all Q branches; for each Q branch there should be a P and an R branch covering at room temperature a range of perhaps ± 20 cm^{-1} on each side.[5] These P and R branches should form a weak penumbra extending (at room temperature) perhaps 15–20 cm^{-1} to higher frequencies outside the p, r head, and also a practically continuous background inside this head.

Henrici and Grieneisen describe the observed B_1 band at very low pressures as about 10 cm^{-1} wide with center at 49,715 cm^{-1}. Scheibe, Povenz, and Linström[10] speak of the band as having a head. In the case of some of the other pseudo-parallel bands, Henrici and Grieneisen also speak of a head. This is true of the 0←1 band of the CH_3 deformation frequency and of the 1←0 band of the $C-I$ frequency, with heads at 48,478 cm^{-1} and 50,223 cm^{-1}, respectively. For the 1←0 (B_2) band of the CH_3 deformation frequency (at 50,805 cm^{-1} according to Henrici and Grieneisen), Scheibe, Povenz, and Linström record a head at 50,810 cm^{-1}. In all these cases, the head is on the ultraviolet side of the band. While the evidence is not wholly clear, it seems to agree within its own uncertainty with the predictions of Eq. (13). Further, Henrici and Grieneisen's observations to the effect that the B_1 band spreads toward both low and high (but especially toward low) frequencies with increase in pressure or temperature seem to be in harmony with expectation. The broadening toward high frequencies beyond the head may be attributed to the penumbra of R branches discussed above.

TABLE II. Bands satellite to B_1 and B_2.

ν	Identification
B_2: 50805	1←0 of CH_3 $\parallel$ deformation vibration
772*	same plus 1←1 of $C-I$ $\parallel$ vibration
741*	same plus 2←2 of $C-I$ $\parallel$ vibration
700	no success in identifying this
B_1: 49721	0←0
687	1←1 of $C-I$ $\parallel$ vibration
652*	2←2 of $C-I$ $\parallel$ vibration
623	no success in identification
581–556 (double?)	581 fits 1←1 of Eq. (14) 560 or 568 fits 1←1 of CH_3 $\parallel$ deformation vibration

* Appears only at high temperature, when also further bands appear at longer wave-lengths than those listed.

Accompanying the B_1 and B_2 bands are weaker bands on the long wave-length side. These become relatively stronger and more numerous at increased temperatures. Table II lists several such bands and our suggested identifications. There are two relatively strong bands (50,700 and 50,623) which we do not see how to explain.

On the high frequency side of B_2 there is a band of wide spacing with every third line strong, similar to those already discussed. This has already been identified[1,2] as a 1←0 band of a degenerate frequency of about 1250 cm^{-1} magnitude corresponding to the infra-red frequency of 1445 cm^{-1}. The seven observed Q frequencies in this band may be expressed by

$$\nu=50{,}942\pm 18K-\tfrac{1}{3}K^2, \qquad (15)$$

but this equation is less reliable than Eqs. (10) and (12). Proceeding as we did above in the case of Eq. (12), we find $\zeta_v'=-0.04$.

On the high frequency side of the band just mentioned, only low dispersion data are available. We shall not discuss these data here, since there is little we could add to existing interpretation. In the region of the lower frequency B bands, although we have discussed all the prominent features, there are some further weak bands, particularly at high temperatures. We shall not attempt to account for these here, since we believe that the nature of the B system is now in general satisfactorily established. The additional weak bands should be explainable by further vibrational transitions, or perhaps in part by vibronic-allowed true parallel transitions (cf. Section 3).

Some of them may arise from transitions to the $[({}^2\Pi_{3/2})\sigma^*]_2$, i.e., ${}^3\Pi_2$ level, which should lie slightly below the $[({}^2\Pi_{3/2})\sigma^*]_1$ level of Eq. (1). Such transitions, although forbidden in first approximation, could occur weakly as a result of spin-orbit coupling together with effects of the C_{3v} symmetry. Possibly the two unidentified bands of Table II belong to this category.

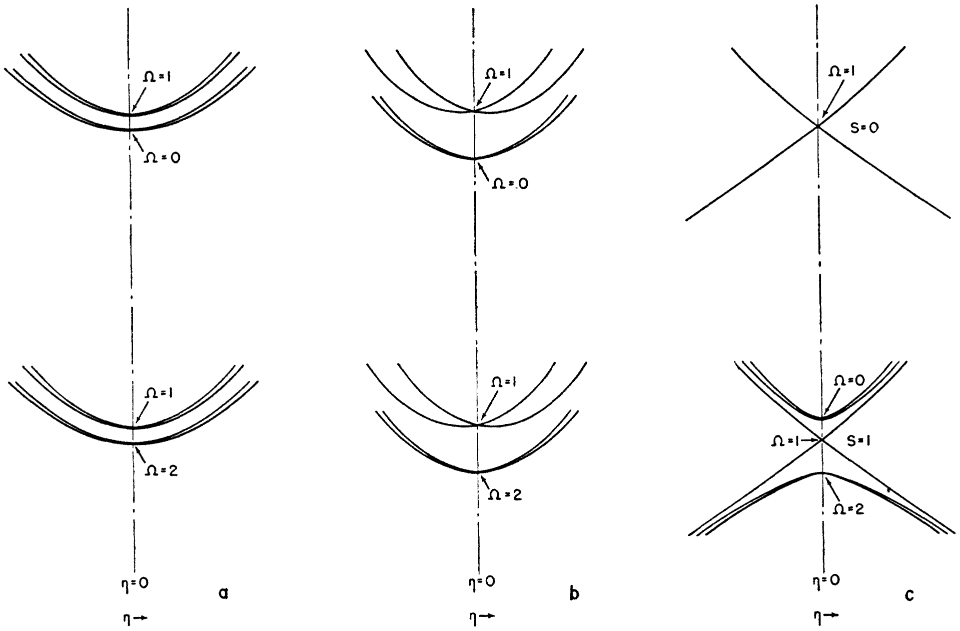

FIG. 3. Energy levels of the methyl iodide *B* and *C* states plotted against the displacement η of an *e*-type vibration. Figure 3a represents the energy levels for *J–j*-like coupling, Fig. 3c for *L–S*-like coupling and Fig. 3b for an intermediate case which corresponds approximately to the actual behavior of methyl iodide.

6. THE INFLUENCE OF SPIN

It has been mentioned in Section 3 that the upper electronic state of the *B* and *C* band systems, which is of *E* type, should be split by *e* type nuclear displacements, and that the equilibrium configuration should not have C_{3v} symmetry. The conclusions in Section 3 were based on the assumption that the splitting of the *E* level is sufficiently small to justify a perturbation treatment in which vibronic states of a model with C_{3v} symmetry serve as unperturbed functions. One important reason for the smallness of the splitting is that the degeneracy of the *E* electronic state is due to a π^3 configuration on the iodine atom and that this part of the molecule is not strongly affected by any *e* vibration. A second reason tending to make the splitting of the *E* level small is the $J-j$-like coupling between spins and orbits in the *B* and *C* states.

In the limiting case of pure $J-j$-like coupling an *e* vibration does not give rise to any linear splitting; i.e., the first-order perturbation energy for the electronic levels in question vanishes. This can be seen in the following way. For pure $J-j$-like coupling the electronic wave function can be written according to (1) as a product of a function characterizing the core ($^2\Pi_{3/2}$ for the *B* state and $^2\Pi_{1/2}$ for the *C* state) and a wave function of the outermost electron σ^*a_1. The core wave function contains the orbital degeneracy. But the number of electrons in the core is odd and the wave function of the core is only twofold degenerate; under these conditions no nuclear displacement can split the wave function of the core.[11] The same holds for the twofold degeneracy of the outermost electron. But for a product wave function the first-order perturbation vanishes if the perturbation is zero for the separate factors.

In Fig. 3a the electronic levels are plotted for $J-j$-like coupling as a function of an *e*-type displacement whose magnitude is measured by the abscissa η. For $\eta=0$ one obtains, as stated in Section 1, two twofold degenerate lower levels belonging to the $\Pi_{3/2}$ core; the Ω values of these levels are 2 and 1. In addition there appear two higher levels belonging to the $\Pi_{1/2}$ core, with

---

[11] For the proof, see H. A. Kramers, Proc. Acad. Sci. Amst. **33**, 595 (1930); E. Wigner, Nachr. Ges. Wiss. Göttingen (1932), p. 546; H. A. Jahn, Proc. Roy. Soc. **164**, 117 (1938).

$\Omega=0$ and $\Omega=1$; for $\Omega=0$ one actually finds two levels with a very small energy difference. The angular momentum Ω is composed of the orbital momentum* Λ, the component along the symmetry axis of the spin of the core, Σ_c, and that of the spin of the outer electron, Σ_σ. In Table III all these momenta are shown for the various electronic states. The first column specifies the core wave function. The last column contains symbols to be used for the wave functions in the subsequent discussion. The splitting of the two $\Omega=0$ levels for $\eta=0$ is not taken into account in the table. If $\eta\neq 0$ the nuclear displacement gives rise to non-diagonal matrix elements between states which differ in the sign of Λ but which agree in the signs of Σ_c and Σ_σ. Thus there are matrix elements between ψ_1 and ψ_{-3}, ψ_{-1} and ψ_3, ψ_2 and ψ_{-4} and finally between ψ_{-2} and ψ_4. In first approximation these matrix elements are proportional to η. It is seen that no matrix elements connect wave functions belonging to the same unperturbed energy. Therefore no splitting occurs which is proportional to the first power of the perturbing potential and therefore to the first power of η. The same result was obtained above by different reasoning. The non-diagonal matrix elements connecting states of different energies, however, give rise to second-order perturbations in the energy and it can be shown that all degenerate levels suffer a splitting proportional to η^2. This splitting is illustrated in Fig. 3a.

For extreme *L*, *S*-like coupling the influence of an *e*-type nuclear displacement is much more important. In Fig. 3c the behavior of the energy levels is illustrated for this case. At $\eta=0$ one finds a $^3\Pi$, with Ω values equal to ± 2, ± 1 and 0. Two levels with slightly different energies belong to the last value. In addition a $^1\Pi(\Omega=\Lambda=\pm 1)$ is found at a higher energy. If η is different from zero and is not very small, the main effect of the *e*-type displacement is a splitting of the $\Lambda=\pm 1$ degeneracy. One finds in the energy region of the original triplet three closely spaced levels whose energies increase linearly with η and three further levels whose energies decrease at the same rate with η. In the energy region of the original singlet one finds two energy levels, one increasing and the other decreasing linearly with η. The energy levels for small η values may be obtained by applying the method of perturbations. In the notation of Table III the triplet wave functions at $\eta=0$ may be written as follows: ψ_1 and ψ_{-1} for $\Omega=\pm 2$, $(1/\sqrt{2})(\psi_2+\psi_4)$ and $(1/\sqrt{2})(\psi_{-2}+\psi_{-4})$ for $\Omega=\pm 1$, ψ_3 and ψ_{-3} for $\Omega=0$. The singlet levels are $(1/\sqrt{2})(\psi_2-\psi_4)$ and $(1/\sqrt{2})(\psi_{-2}-\psi_{-4})$. The nuclear displacement gives rise to matrix elements between the degenerate pair of wave functions $(1/\sqrt{2})(\psi_2+\psi_4)$ and $(1/\sqrt{2})(\psi_{-2}+\psi_{-4})$ and also between the degenerate pair $(1/\sqrt{2})(\psi_2-\psi_4)$ and $(1/\sqrt{2})(\psi_{-2}-\psi_{-4})$. Therefore the first-order perturbation energy does not vanish for these pairs of levels, and these levels suffer a splitting which increases linearly with η. Further matrix elements occur between ψ_1 and ψ_{-3} and between ψ_{-1} and ψ_3. In this case the first-order perturbation vanishes but the small energy difference of the interacting levels brings about a large perturbation energy of the second order. For this reason the highest and lowest pair of potential energy curves of the triplet are sharply bent near $\eta=0$.

With increasing η the non-diagonal matrix elements between ψ_1 and ψ_{-3}, and between ψ_{-1} and ψ_3, become large compared with the splitting of the triplet at $\eta=0$. Then the highest and lowest potential curves of the triplet approach the middle curve. Figure 3c shows furthermore that the potential curves do not intersect anywhere except at $\eta=0$.

In Fig. 3b an intermediate case between pure

TABLE III. Angular momenta and symbols of wave functions for perfect *J–j*-like coupling.

	Ω	Λ	Σ_c	Σ_σ	
$\Pi_{-1/2}$	-1	-1	$\frac{1}{2}$	$-\frac{1}{2}$	ψ_{-4}
$\Pi_{1/2}$	1	1	$-\frac{1}{2}$	$\frac{1}{2}$	ψ_4
$\Pi_{-1/2}$	0	-1	$\frac{1}{2}$	$\frac{1}{2}$	ψ_{-3}
$\Pi_{1/2}$	0	1	$-\frac{1}{2}$	$-\frac{1}{2}$	ψ_3
$\Pi_{-3/2}$	-1	-1	$-\frac{1}{2}$	$\frac{1}{2}$	ψ_{-2}
$\Pi_{3/2}$	1	1	$\frac{1}{2}$	$-\frac{1}{2}$	ψ_2
$\Pi_{-3/2}$	-2	-1	$-\frac{1}{2}$	$-\frac{1}{2}$	ψ_{-1}
$\Pi_{3/2}$	2	1	$\frac{1}{2}$	$\frac{1}{2}$	ψ_1

---

* On account of the C_{3v} symmetry, Ω and Λ do not have exactly integral values. In the following we shall consider the limiting case in which $\Lambda=1$ and $\Lambda=-1$ for the electronic functions E^+ and E^-. The argument would not lose its validity for non-integral values of Λ and Ω but in that case a somewhat more cumbersome notation would be necessary. Here and in the following discussion we shall attach *signs* to Λ and Ω, although as ordinarily defined these symbols refer to absolute values; we shall likewise use Σ with signs defined relative to the positive direction along the symmetry axis.

$L-S$-like and pure $J-j$-like coupling is represented. Corresponding to the actual properties of CH_3I the coupling shown in Fig. 3b is closer to the $J-j$-like than to the $L-S$-like coupling. For $\eta=0$ two pairs of levels occur with $\Omega=\pm2$, ±1 in the lower pair, and $\Omega=0$, ±1 in the upper pair. The wave functions belonging to $\Omega=\pm2$ and $\Omega=0$ for $\eta=0$ are the same for pure $L-S$-like coupling, pure $J-j$-like coupling, and for all intermediate couplings. In the wave functions of the lower $\Omega=\pm1$ levels in Fig. 3b ψ_2 and ψ_{-2} predominate, but a small admixture of ψ_4 and ψ_{-4} is present. The wave functions may be written in the form $\psi_2+\epsilon\psi_4$ and $\psi_{-2}+\epsilon\psi_{-4}$. Here ϵ is a number smaller than unity; the normalization factor has been omitted. In the upper levels with $\Omega=\pm1$ the main parts of the wave functions are ψ_4 and ψ_{-4}; the functions ψ_2 and ψ_{-2} appear with small negative coefficients. The wave functions are $\psi_4-\epsilon\psi_2$ and $\psi_{-4}-\epsilon\psi_{-2}$. For $\eta\neq0$ matrix elements exist between the $\Omega=\pm2$ and the $\Omega=0$ levels. This gives rise to quadratic perturbations in the energy. The perturbations are not very large, because of the relatively great distance between the levels concerned. At the same time, matrix elements appear between the lower $\Omega=1$ and the upper $\Omega=-1$ levels, and also between the lower $\Omega=-1$ and the upper $\Omega=1$ levels. These matrix elements cause quadratic perturbations similar to those affecting the $\Omega=\pm2$ and $\Omega=0$ levels. But because of the admixture of ψ_4 and ψ_{-4} functions in the lower $\Omega=\pm1$ level, smaller matrix elements appear between the lower $\Omega=1$ state and the $\Omega=-1$ belonging to the same energy. For small ϵ values, these matrix elements differ from the matrix elements mentioned above by a factor ϵ. As a consequence, a small first-order perturbation in the energy is obtained, and the splitting of the $\Omega=\pm1$ level varies linearly with η for small η values. The same holds for the upper $\Omega=\pm1$ level. Here the splitting is caused by the admixture of the ψ_2 and ψ_{-2} functions, which gives rise to small matrix elements between the upper $\Omega=1$ state and the $\Omega=-1$ state of the same energy. In Section 3 we had assumed a small linear splitting of the $\Omega=\pm1$ degenerate levels. Our present results justify that assumption.

The above discussion has a direct bearing on the intensity of the $1\leftarrow0$ and $0\leftarrow1$ transitions of an e-type vibration in the B band system. The $1\leftarrow0$ transition is made possible by admixture between the vibrationless electronic state E^- and the vibronic state E^+e^+ (and similarly by the admixture of E^+ with E^-e^-). Now the E^+e^+ state of the B system interacts with the vibrationless E^- state of the C system. This is due to the matrix element appearing for $\eta\neq0$, between the $\Omega=1$ state of the B system and the $\Omega=-1$ state of the C system. As a result the wave function $\psi_{-4}-\epsilon\psi_{-2}$ is admixed with the original function $\psi_2+\epsilon\psi_4$. The amount of this mixing is proportional to the matrix element and inversely proportional to the energy difference between the E^+e^+ level of the B system and the E^- level of the C system.

The E^+e^+ vibronic state of the B system also interacts with the E^- state of the same system. This interaction is due to the smaller matrix elements arising for $\eta\neq0$ between the $\Omega=1$ and $\Omega=-1$ states of the B system. As a result the wave function $\psi_{-2}+\epsilon\psi_{-4}$ is admixed with the original function $\psi_2+\epsilon\psi_4$. The amount of the mixing is proportional to the matrix element between the $\Omega=1$ and $\Omega=-1$ states of the B system: this matrix element is smaller than the one mentioned in the previous paragraph by roughly the factor ϵ. But the mixing is also inversely proportional to the energy difference between the E^+e^+ level and the E^- level of the B system. This energy difference is about five times smaller than the energy difference referred to in the last paragraph. Thus it is possible that the E^- states of the B system and the C system are admixed with the E^+e^+ state of the B system with coefficients of a similar magnitude.

The matrix element of the electric dipole causing the $1\leftarrow0$ transition of the B system is a sum of the dipole matrix elements due to the admixture of the E^- states of the B and C systems. The interference of these two dipole matrix elements must therefore be taken into account. The energy difference between E^+e^+ of the B system and E^- of the same system is positive. The energy difference between E^+e^+ of the B system and E^- of the C system is negative. This causes a difference in sign in the admixtures of the E^- function of the B system and the E^- function of the C system. On the other hand, the dipole matrix elements leading from the ground state to the E^- states of the B and the C system differ in sign. Indeed the largest term in the E^- wave function of the B system is ψ_{-4} while that in the E^- wave function of the C system is ψ_{-2}. Now $\psi_{-4}+\psi_{-2}$ is the wave function of a pure triplet state which does not combine with the ground state. Therefore the dipole matrix elements leading to ψ_{-4} and to ψ_{-2} must differ by a factor -1. Since the matrix elements leading to the E^- states of the B and C system differ in sign and since these E^- states are admixed with opposite signs into the E^+e^+ state, it follows that a constructive interference exists between the contributions of the two E^- states to the intensity of the 1←0 transition.

The 0←1 transition of the 880 cm^{-1} vibration is made possible by the admixture of E^+e^+ states of the B and the C system with the vibrationless E^- state of the B system. Arguments similar to those given above can be used to find out whether the contributions of the two E^+e^+ states to the dipole matrix element tend to reinforce or to cancel each other. A difference from the previous reasoning arises in one point: while in the above discussion the E^+e^+ state lay between the two E^- states, in the present case the E^- state of the B system lies lower than either of the two E^+e^+ states. Consequently the two E^+e^+ states are admixed into the E^- state with the same sign. The dipole matrix elements leading from the vibrating electronic ground state to the two E^+e^+ states are of opposite signs. This is true for the same reason for which the matrix elements leading from the ground state of the molecule to the E^- states differ in sign. The result is that the interference between the two E^+e^+ states contributing to the dipole matrix element of the 0←1 transition is destructive.

The data published by Henrici and Grieneisen[2] contain indications that the 0←1 transition probability of the 880 cm^{-1} vibration is smaller than the 1←0 transition of the corresponding vibration. If one assumes that the intensities are roughly proportional to the vapor pressures at which the 0←1 and 1←0 bands appear, one finds that at 300°K the 0←1 band is 300 or 400 times less intense than the 1←0 band. If the intensity ratio were due to the Boltzmann factor arising from the thermal excitation of an 880 cm^{-1} quantum in the 0←1 transition, the ratio would be 65. The larger intensity ratio of 300 or 400 indicates that the 0←1 transition is weakened by the destructive interference discussed above. The same conclusion is reached from intensity measurements at 600°K. Here the 1←0 and 0←1 bands have the apparent intensity ratio of 60, which is to be compared with a Boltzmann factor of 8. But the existing intensity measurements in the B system of methyl iodide are not sufficiently accurate to justify a comparison between experiment and the quantitative consequences of the previous paragraphs. If accurate measurements were available, such a comparison could be utilized to obtain information about the quantity ϵ which measures the deviation from pure $J-j$-like coupling.